RSC Advances



This is an *Accepted Manuscript*, which has been through the Royal Society of Chemistry peer review process and has been accepted for publication.

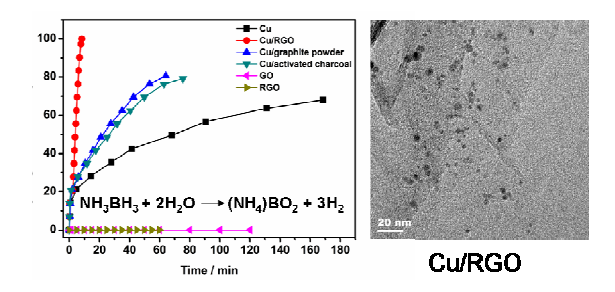
Accepted Manuscripts are published online shortly after acceptance, before technical editing, formatting and proof reading. Using this free service, authors can make their results available to the community, in citable form, before we publish the edited article. This Accepted Manuscript will be replaced by the edited, formatted and paginated article as soon as this is available.

You can find more information about *Accepted Manuscripts* in the **Information for Authors**.

Please note that technical editing may introduce minor changes to the text and/or graphics, which may alter content. The journal's standard <u>Terms & Conditions</u> and the <u>Ethical guidelines</u> still apply. In no event shall the Royal Society of Chemistry be held responsible for any errors or omissions in this *Accepted Manuscript* or any consequences arising from the use of any information it contains.



Colour Graphical



A facile in situ procedure has been successfully applied for synthesis of a RGO-Cu nanocomposites, which leads to the highest catalytic activity of Cu nanocatalysts up to now toward the dehydrogenation of ammonia borane.

Journal Name

RSCPublishing

COMMUNICATION

Cite this: DOI: 10.1039/x0xx00000x

Facile in situ synthesis of copper nanoparticles supported on reduced graphene oxide for hydrolytic dehydrogenation of ammonia borane

Received 00th January 2012, Accepted 00th January 2012

DOI: 10.1039/x0xx00000x

www.rsc.org/

Yuwen Yang, ^a Zhang-Hui Lu, ^{a*} Yujuan Hu, ^a Zhujun Zhang, ^a Weimei Shi, ^{b*} and Xiangshu Chen, ^{a*} Tingting Wang^a

Reduced graphene oxide (RGO) supported copper nanoparticles (NPs) were synthesized via a facile in situ procedure using ammonia borane (AB) as a reductant. The as-prepared nanocatalysts exert satisfied catalytic activity (3.61 mol H₂ mol catalyst⁻¹ min⁻¹), which appears to be the best Cu nanocatalysts up to now toward the dehydrogenation of ammonia borane.

Ammonia-borane (AB, NH₃BH₃) nontoxic, environmentally benign, and is considered to be an attractive solid hydrogen storage materials due to its high hydrogen mass capacity, high solubility and demonstrated stability in neutral aqueous solutions [1]. With appropriate catalyst, catalytic hydrolysis of AB can release three mol of H₂ per mol AB at room temperature, which appears to be the most convenient one for portable hydrogen storage applications [2]. So far, not only noble [2-8] and non-noble metal NPs [9-24], but also their composites have been explored for hydrolytic dehydrogenation of AB. The noble metal-based catalysts exhibit a higher catalytic activity, but they are unsuitable for practical applications due to their limited resources and high price tags. Therefore, the development of efficient and economical nonnoble catalysts is of great importance for the practical application of the hydrogen generatin/storage systems. Copper (Cu), an abundant element in the earth's crust, has been studied as the catalyst in dehydrogenation reactions. Unfortunately, Cu nanocatalysts are found just to be modesty active for hydrolytic dehydrogenation of AB up to now [8,10,14-18,25]. For this reason, achieving the high activity of Cu nanocatalysts is of great practical and scientific interest.

Graphene, a new class of two-dimensional carbon nanostructure with one-atom thickness, holding many advantages such as outstanding charge carrier mobility [26], thermal and chemical stability [27], high specific surface area [28], and superior electrical conductivity [29], etc., could be an ideal substrate for growing and anchoring metal NPs with good dispersion. In this work, the RGO

supported Cu NPs were prepared within a few minutes by the in situ chemical reduction of mixture containing graphene oxide (GO) nanosheets and Cu(II) ions using AB as a reductant. The as-prepared RGO supported Cu NPs exhibit a high catalytic activity for hydrogen generation from the aqueous of AB at room temperature.

In brief, the *in situ* synthetic and catalytic procedure was achieved by adding AB into the precursor solution containing graphene oxide (GO) nanosheets and $CuSO_4$, and the gas generated was measured volumetrically. The Cu^{2+} with high reduction potentials ($E^0Cu(II)/Cu(I) = +0.159$ eV vs. SHE; $E^0Cu(I)/Cu = +0.520$ eV vs. SHE)) was firstly reduced by AB, and then the generated active intermediate Cu-H species with a strong reducing ability can further reduce the GO although they can not be directly reduced by AB. The detailed experimental process could be found in the supplementary material.

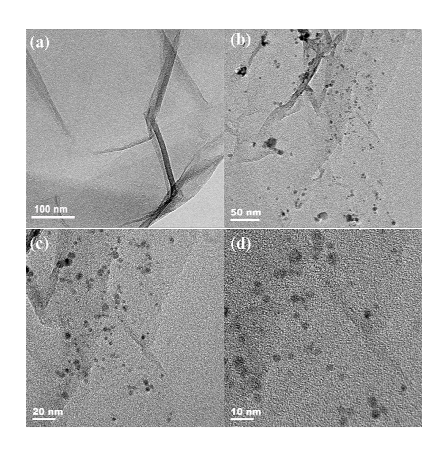


Fig. 1 TEM images of GO nanosheets (a) and Cu/RGO (b-d).

The microstructure of the obtained samples was characterized by transmission electron microscopy (TEM). As shown in Fig. 1(a), the GO nanosheets are transparent and corrugated together. The TEM images of Cu/RGO nanocatalysts (Fig. 1b-1d) show that most

Page 3 of 5 COMMUNICATION Journal Name

RSC Advances

of the Cu NPs lay flat on the RGO, with some possessing folded edges exhibiting parallel lines. The ultrafine Cu NPs were wrapped by RGO sheets, which could help to prevent Cu from agglomeration.

The phase structure and purity of Cu/RGO was characterized by X-ray diffraction (XRD) (Fig. 2a). The diffraction peaks (2θ) of Cu/graphene at 43.2°, 50.2°, 74.1° and 89.9° are ascribed to the (111), (200), (220), (311) planes of Cu NPs, which are similar to those of cubic Cu (JCPDS No. 04-0836). The weak peak at around 36.20° is stand for oxidized Cu, which is due to the partly surface oxidation of Cu NPs and could not be avoided. The most intense peak at around $2\theta = 11.59^{\circ}$ corresponds to the (001) reflection of GO disappeared, while a new peak at around 25.06° is observed in the as-prepared Cu/RGO, indicating that GO is successfully reduced to graphene.

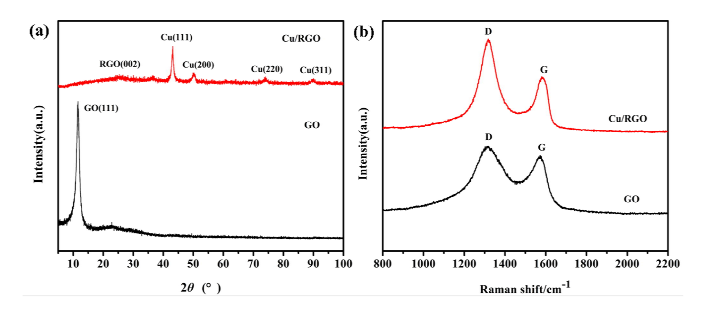


Fig. 2 (a) XRD patterns and (b) Raman spectra of the GO (black) and Cu/RGO (red).

Two peaks centered at 1317 and 1577 cm-1 appear in the Raman spectra of the GO and RGO supported Cu NPs (Fig. 2b), corresponding to the D and G bands of the carbon products, respectively. The intensity ratio of the D to G band (I_D/I_G) is generally accepted to reflect the degree of graphitization of carbonaceous materials and defect density. After loading of the Cu NPs, the I_D/I_G of GO is increased from 1.1 to 1.6. The relative changes in the D to G peak intensity ratio confirm the reduction of GO during the in situ fabrication.

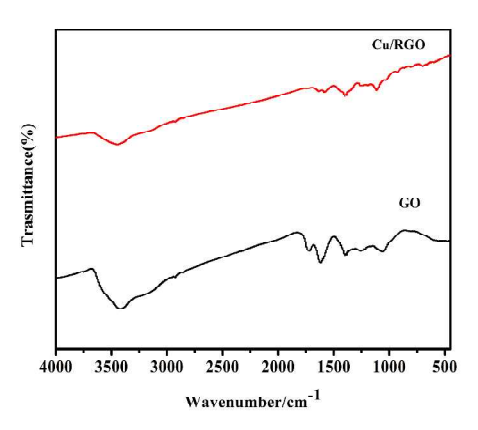


Fig. 3 FTIR spectra of the GO (black) and Cu/RGO (red).

The FTIR spectra of GO and Cu/RGO NPs are shown in Fig. 3. In the spectrum of GO, the broad and intense band at 3419.8 cm⁻¹ was ascribed to the hygroscopicity of GO. The weak band at 1716.1 cm⁻¹ was assigned to C=O stretching vibration in carbonyl or carboxylic groups. The peak at 1619.4 cm⁻¹ was pertinent to the vibrations of the absorbed water molecules and the skeletal vibration of unoxidized graphitic domains. The bands at 1399.0 and 1064.4 cm⁻¹ were associated with the O-H vibration in carboxyl acid and the deformation of the C-O band respectively. The disappearance of C=O, C-OH and C-O of GO after the formation of the RGO supported Cu NPs, further indicates that the GO was reduced to the graphene during the process. The XPS characterizations confirmed that GO and Cu(II) anions were reduced by AB (Fig. S1 and S2). Moreover, after the CuSO₄ and GO reduced by AB, the Cu concentration in the filtrate after removing the RGO along with attached Cu is negligible (0.165 ppm by ICP), compared to the initial 667.1 ppm of Cu²⁺ before the reduction experiment. This confirms that Cu²⁺ was completely reduced to Cu(0).

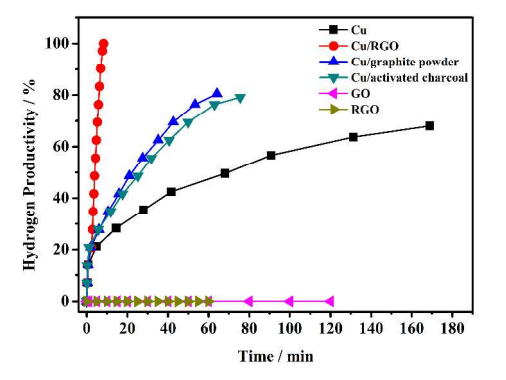


Fig. 4 Hydrogen generation from hydrolysis of ammonia borane (0.10M, 10 mL) in the presence of Cu, Cu/RGO, Cu/activated charcoal, Cu/graphite powder, GO and RGO. (Cu/AB=0.1).

The catalytic activity of the as-synthesized Cu/RGO for hydrolytic dehydrogenation of AB at room temperature is presented in Fig. 4, compared with those of Cu/gtaphite, Cu/activated charcoal, support-free Cu NPs, GO and RGO. No hydrogen generation were observed for GO and RGO, suggesting that GO and RGO have no catalytic activity for the hydrolysis of AB. The hydrogen productivity from AB catalyzed by pure Cu NPs is around 66.67%. RGO, graphite powder, and activated charcoal supported Cu NPs show the better activity than pure Cu NPs. Especially, Cu/RGO generate a stoichiometric amount of hydrogen ($H_2/NH_3BH_3 = 3.0$) in 8.3 min with a turnover frequency (TOF) value of 3.61 mol H₂ mol catalyst⁻¹ min⁻¹, which is the highest one among all of the Cu nanocatalysts ever reported for this reaction (Table S1). Moreover, compared with RGO mixed with Cu NPs, the as-synthesized Cu/RGO exhibit superior catalytic performance (Fig S3). In addition, this catalyst shows a good recycle stability, even after 4 runs, the productivity of hydrogen remained almost unchanged (Fig. S4). The Cu concentration in the filtrate after removing Cu/RGO catalysts was measured to be 0.416 ppm by ICP, indicating that most of copper NPs still remain on RGO after the cycle test. The enhanced catalytic activity of Cu/RGO for AB hydrolysis reaction should result from the cooperative effect between RGO and Cu NPs, which is mainly caused by the charge transfer across the graphene-copper interface due to the graphene-copper spacing and Fermi lever difference.

RSC Advances Page 4 of 5 Journal Name **COMMUNICATION**

Table 1 The values of activation energy (E_a) for hydrolysis of AB Furthermore, this simple synthetic method can be extend to catalyzed by different catalysts.

Catalyst	$E_{\rm a}({\rm kJ/mol})$	Ref.
Ni powder	70	[12]
Zeolite stabilized Rh	67	[5]
$\text{Co}/\gamma\text{-Al}_2\text{O}_3$	62	[9]
Intrazeolite Co(0) nanoclusters	56	[23]
Zeolite-confined Cu	51.8±1.8	[16]
NiAg	51.5	[13]
Cu _{0.2} @Co _{0.8} /graphene	51.3	[19]
Pd/graphene	51	[7]
Ru/carbon black (CB)	49.18	[6]
p(AMPS)-Cu	48.8	[15]
$Cu_{0.33}Fe_{0.67}$ alloys	43.2	[10]
Ni _{0.35} Pt _{0.65} alloys	39	[14]
Cu/RGO	38.2±1.5	This study
Pt/γ - Al_2O_3	21	[3]

A series of experiments was carried out explore the kinetics of the dehydrogenation of AB.Fig. S6(a) shows a plot of the hydrogen generated versus time during the catalytic hydrolysis of AB with different Cu concentration. When the Cu concentration increased, the reaction time decreased obviously. The hydrogen generation rate was determined from the linear portion of the plot for each Cu concentration. Fig. S6(b) shows the plot of hydrogen generation rate versus Cu/RGO concentration on a logarithmic scale. A slope of 1.13 in the inset indicates that the hydrolysis catalyzed by Cu/RGO is first-order in catalyst concentration. In order to get the activation energy (E_a) of the AB hydrolysis catalyzed by Cu/RGO, the hydrolytic reaction at different temperature range of 298-313 K were carried out. The values of rate constant k at different temperatures were calculated from the slope of the linear part of each plot from Fig. S7(a). The Arrhenius plot of ln k vs. 1/T for the catalyst is plotted in Fig. S7(b), from which the apparent activation energy was determined to be approximately 38.2 ± 1.5 kJ/mol. which is lower than most of the reported activation energy values for the same reaction using non-noble metal catalysts and even some noble metal based catalysts (Table 1) [3,5-7,9,10,12-16,19,25].

In summary, we have developed a facile in situ one-step method for the synthesis of graphene supported Cu NPs using AB as a reducing agent within a few minutes at room temperature. The RGO supported Cu NPs exhibit higher catalytic activity than the activated charcoal and graphite power supported or RGO free (Cu NPs) counterparts towards the hydrolytic dehydrogenation of AB. The RGO proved to be a distinct and powerful support for Cu-based catalyst.

other RGO-based metallic systems in more applications.

Acknowledgement

This work was financially supported by National Natural Science Foundation of China (No. 21103074), Natural Science Foundation of Jiangxi Province of China (No. 20114BAB203010 and 20132BAB203014), Jiangxi Provincial Department of Science and Technology (No. 20111BDH80023) and Scientific Research Foundation of Graduate School of Jiangxi Province (YC2013-S105). Z.-H. Lu was supported by the Sponsored Program for Cultivating Youths of Outstanding Ability in Jiangxi Normal University, Young Scientist Foundation of Jiangxi Province (20133BCB23011), and "Gan-po talent 555" Project of Jiangxi Province.

Notes and references

^aCollege of Chemistry and Chemical Engineering, Jiangxi Normal University, E-mail Nanchang, 330022, China. address: luzhanghui@hotmail.com (Z.-H. Lu); cxs66cn@jxnu.edu.cn (X. Chen); Fax: +86 791 88120843; Tel: +86 791 88121974 ^bSichuan research center of new materials, Institute of Chemical Materials, China Academy of Engineering Physics, Mianyang, 621900, China. E-mail address: shiweimei82@gmail.com (W. Shi)

Electronic Supplementary Information (ESI) available: materials, methods, supplementary figures and table. See DOI: 10.1039/c000000x/

- [1] Z. H. Lu and Q. Xu, Funct. Mater. Lett., 2012, 5, 1230001.
- [2] M. Chandra and Q. Xu, J. Power Sources, 2006, 156, 190-194.
- [3] M. Chandra and Q. Xu, J. Power Sources, 2007, 168, 135-142.
- [4] Z. H. Lu, H. L. Jiang, M. Yadav, K. Aranishi and Q. Xu, J. Mater. Chem., 2012, 22, 5065-5071.
- [5] S. Basu, A. Brockman, P. Gagare, Y. Zheng, P. V. Ramachandran, W. N. Delgass and J. P. Gore, J. Power sources, 2009, 188, 238-243.
- [6] G. Z. Chen, S. Desinan, R. Rosei, F. Rosei and D. L. Ma, Chem. Eur. J., 2012, 18, 7925-7930.
- [7] P. X. Xi, F. J. Chen, G. Q. Xie, C. Ma, H. Y. Liu, C. W. Shao, J. Wang, Z. H. Xu, X. M. Xu and Z. Z. Zeng, Nanoscale, 2012, 4, 5597-5601.
- [8] Q. L. Yao, W. M. Shi, G. Feng, Z. H. Lu, X. L. Zhang, D. J. Tao, D. J. Kong and X. S. Chen. J. Power Sources, 2014, doi: 10. 1016/j.jpowsour. 2014.01.122.
- [9] Q. Xu and M. Chandra, J. Power Sources, 2006, 163, 364-370.
- [10] Z. H. Lu, J. P. Li, A. L. Zhu, Q. L. Yao, W. Huang, R. Y. Zhou, R. F. Zhou and X. S. Chen, Int. J. Hydrogen Energy, 2013, 38, 5330-5337.
- [11] S. B. Kalidindi, M. Indirani and B. R. Jagirdar, Inorg. Chem., 2008, 47, 7424-7429.
- [12] F. Y. Cheng, H. Ma, Y. M. Li and J. Chen, Inorg. Chem., 2007, 46, 788-
- [13] C. F. Yao, L. Zhuang, Y. L. Cao X. P. Ai and H. X. Yang, Int. J. Hydrogen Energy, 2008, 33, 2462-2467.
- [14] X. J. Yang, F. Y. Cheng, J. Liang, Z. L. Tao and J. Chen, Int. J. Hydrogen Energy, 2009, 34, 8785-8791.
- [15] O. Ozay, E. Inger, N. Aktas and N. Sahiner, Int. J. Hydrogen Energy 2011, 36, 8209-8216.

RSC Advances COMMUNICATION Journal Name

- [16] M. Zahmakıran, F. Durap and S. Özkar, Int. J. Hydrogen Energy, 2010, **35**, 187-197.
- [17] M. Kaya, M. Zahmakiran, S. Özkar and M. Volkan, ACS Appl. Mater. Interfaces, 2012, 4, 3866-3873.
- [18] J. M. Yan, Z. L. Wang, H. L. Wang and Q. Jiang, J. Mater. Chem., 2012, 22, 10990-10993.
- [19] Y. S. Du, L. Yang, N. Cao, W. Luo and G. Cheng, New J. Chem., 2013, 37, 3035-3042.
- [20] S. B. Kdlidindi, U. Sanyal and B. R. Jagirdar, Phys. Chem. Chem. Phys., 2008, 10, 5870-5874.
- [21] Y. Yamada, K. Yano, Q. Xu and S. Fukuzumi, J. Phys. Chem. C, 2010, **114**, 16456-16462.
- [22] Y. Yamada, K. Yano and S. Fukuzumi, Energy Environ. Sci., 2012, 5, 5356-5363.
- [23] M. Rakap and S. Özkar, Int. J. Hydrogen Energy., 2010, 35, 3341-3346.
- [24] J. M. Yan, X. B. Zhang, S. Han, H. Shioyama and Q. Xu, Angew. Chem. Int. Ed. Engl. 2008, 47, 2287-2289.
- [25] Z. H. Lu, Q. L. Yao, Z. J. Zhang, Y. W. Yang, X. S. Chen, J. Nanomater 2014, 729029.
- [26] C. Lee, X. D. Wei, J. W. Kysar and J. Hone, Science, 2008, 321, 385-388.
- [27] K. S. Novoselov, A. K. Geim, S. V. Morozov, Y. Zhang, S. V. Dubonos,
- I. V. Grigorieva and A. A. Firsov, Science, 2004, 306, 666-669.
- [28] S. Garaj, W. Hubbard, A. Reina, J. Kong, D. Branton, J. A. Golovchenko, Nature, 2010, 467, 190-194.
- [29] B. G. Choi, J. Hong, Y. C. Park, D. H. Jung, W. H. Hong, P. T.
- Hammond and H. S. Park, ACS Nano 2011, 5, 5167-5174.